Journal of Electrostatics 126 (2023) 103866

Contents lists available at ScienceDirect

Journal of Electrostatics

journal homepage: www.elsevier.com/locate/elstat

Full length article

Capacitance of a conducting hollow cylindrical shell in a closed form

E. Romashets [a,*], M. Vandas [b], C. Şen [a]

[a] Lamar University, Department of Physics, PO, Beaumont, 8832, TX, USA
[b] Astronomical Institute of the Czech Academy of Sciences, Prague, Czech Republic

ARTICLE INFO

Keywords:
Electrostatic potential
Electrostatic energy

ABSTRACT

The charge distribution within a hollow conducting cylinder with zero-thickness walls is calculated from the minimum potential energy (U) consideration. The surface charge density consists of a diverging term (Jackson, 1975) and a sum of Legendre polynomials with the coefficients determined from the minimum U approach. The sum converges. This allows to express the capacitance in closed form. It is in agreement with Butler (1980). We present electric field lines inside and outside of the cylinder. An electric field pattern can be studied in detail. Most of the numerical analysis is done for the conducting cylinder of the length equal to ten radii. The surface charge density near the edges diverges; and in the middle, it is twenty five percent less than that of a uniformly distributed charge. The self-energy of the conducting cylinder is about 5 percent lower than that of uniformly distributed surface charge.

1. Introduction

Landau and Lifshitz [1] found the electric field of charged conducting oblate and prolate ellipsoids of rotation. Recently, the half-sphere capacitance has been solved [2]. The analysis of equally distributed charges of various finite but not whole surfaces can be found in the literature [3,4]. It is interesting that the one-dimensional problem of finding equilibrium charge distribution on a finite straight wire has not been solved so far [5–7]. The study of a hollow conducting cylinder of zero thickness, as it is depicted in Fig. 1, can clarify the charge on the wire problem. Conducting cylinders have attracted vast attention from scientists and various important results have been published in a variety of studies. Bruno and Brauder [8] used the finite element analysis to calculate the scattering of electromagnetic waves from an infinite as well as from a finite conducting cylinder. Current carrying truncated cylindrical regions and their resulting electrical and magnetic properties have been investigated numerically and it has been found that the results depend significantly on the length of the cylindrical target [9]. Effects of point charges near an infinite conducting cylinder have been evaluated using the Green's function method. It has been shown that the net force on the point charge goes to zero as the radius of the cylinder approaches zero, regardless of the distance of the external point charge to the conducting line [10]. Sharstein [11] looked at the electrostatic problem of a hollow, conducting tube of a finite length held at a constant potential. In another study, Weinheimer [12] looked into the charge induced by a point charge on conducting cylinder. The location of the point charge was varied and numerical results were presented. In addition to electromagnetic properties, Buikis and Kalis [13] also investigated the force and temperature distribution in a finite cylinder.

In [14], the charge on conducting cylinder was found from the constant voltage V_0 on the surface of the cylinder, in the form of an infinite sum of terms with singularities on the edges. Earlier works on this approach are reviewed in [15]. The main advances were made by Kapitsa et al. [16], Vainshteyn [17], Lebedev and Skalskaya [18], and Butler [19]. The idea was to write an electric potential on the surface as an integral which is decomposed into a Fourier series. The resulting charge density, σ, is a sum of the orthogonal functions along with corresponding coefficients. Each function contains $\frac{1}{\sqrt{1-\frac{2z}{L}}}$, where L is the length and z is the position along the axis of the cylinder (see Fig. 1). The charge density as well as the electric field magnitude near the edges of the cylinder diverge as $\frac{1}{\sqrt{d}}$, where d is the distance from the edge. The highly fluctuating polynomials in the sum provide that the condition for electric potential to be constant is met for $N = 3$, that is with four terms, $n = 0, 1, 2$, and 3, with precision of the order of a fraction of a percent. Higher precision can be achieved by the increase of N to 6, but dealing with larger Ns brings additional numerical instabilities. This is why a smaller N is preferable. The sum can be adjusted slightly by applying the least squares method instead of the orthogonality method, where only a few first terms are kept in the sum. On the other hand, a few first terms with adjusted coefficients provide the best agreement with the restrained condition in the least squares

* Corresponding author.
E-mail address: eromashets@lamar.edu (E. Romashets).

https://doi.org/10.1016/j.elstat.2023.103866
Received 12 July 2023; Received in revised form 2 November 2023; Accepted 3 November 2023
Available online 8 November 2023

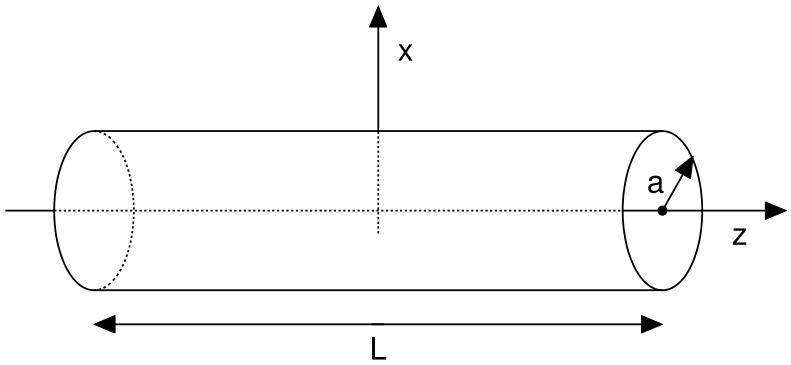

Fig. 1. The view of hollow conducting cylinder of zero thickness.

method. Verolino [14] sum adjusted in this way still demonstrates a relatively large deviation from V_0 on the cylinder. One may think that the much earlier approach proposed by Maxwell [20], in searching the charge density distribution as a sum of finite polynomials, can lead to better results. But it cannot work if the resulting distribution is actually singular on the edge [21]. We propose using Legendre polynomials along with the Jackson [21] term in order to construct the surface charge density on the hollow cylinder of radius a and length L. This will open the way to considering a full cylinder and approaching the limit $a/L \to 0$, corresponding to the straight wire. We use a cylindrical coordinate system r, φ, z. Here, z is the axis of symmetry of the cylinder. The origin is in the middle of the cylinder, at $z = 0$ and $r = 0$. Its radius is a. We treat a cylinder with zero thickness. The cylinder has a length, L, without a base nor top, as shown in Fig. 1. Because of cylindrical symmetry, the charge density is a function of only the position along the cylinder. The natural next step here is to separate the infinite and finite parts in the function to be found, that is one part of the surface charge density σ will contain $\frac{1}{\sqrt{1-\left(\frac{2z}{L}\right)^2}}$ and another one is the sum of finite orthogonal polynomials with their coefficients. This is the novelty of our approach

The least squares method usually means to minimize the deviation from the theoretical or postulated value. But it can also be used to find the minimum potential energy state. Hitherto, all efforts have been applied to solving the constant voltage problem, but no one has attempted to consider a minimum potential self-energy before.

In this work, we choose to expand the finite part of the charge distribution $\sigma(z)$ in Legendre polynomials so as to provide the minimum self-energy. Details are given in Appendix. The result is that for a specific ratio of the radius of the cylinder to its length equal to 0.1, the deviation is comparable to that of the $V = V_0$ approach, with the same number of coefficients. It should be noted that for the minimum self-energy U state, the condition $V = V_0$ is met in the natural way. This exact and compact solution for σ, and hence for electric potential and electric field opens the way to detailed electric field analysis, inside and outside of the cylinder, closer to the edges. We note that the voltage with a larger number in the sum for the charge density approaches a closed form, which can be identified and used for the calculation of capacitance. This paper is organized in the following manner. Section 2 describes the $U = U_{\min}$ method, while specific calculation details are moved to Appendix. Section 3 outlines the results in terms of σ, V, capacitance C, and self-energy U. Special attention is paid to the value of σ in the midpoint of the axis of the cylinder for a different $\xi = \frac{a}{L}$. There are only two coefficients which contribute to the total charge, one near $\frac{1}{\sqrt{1-\mu^2}}$, where $\mu = \frac{2z}{L}$ and one near the Legendre polynomial $P_0(\mu) = P_0\left(\frac{2z}{L}\right) = 1$. The ratio between the two and how it depends on ξ is analyzed as well. The electric field components, contour-plots of its magnitude, and the field-lines are depicted as well. The closed form of capacitance is presented in Section 4. Conclusions are provided in Section 5.

2. Model

Total electrostatic potential energy of a charge distribution is given by

$$U = \frac{1}{2}k\int_Q\int_{Q'}\frac{\mathrm{d}Q\,\mathrm{d}Q'}{|\boldsymbol{r}-\boldsymbol{r}'|}. \tag{1}$$

Here, k is the Coulomb constant, $\boldsymbol{r}$ is the position of the incremental charge $\mathrm{d}Q$, while $\boldsymbol{r}'$ is the position of $\mathrm{d}Q'$.

The integration is over the surfaces A and A', of surface charge densities $\sigma(z)$ and $\sigma(z')$. Since the cylinder has a zero thickness, the surfaces A and A' are identical. The cylinder is of length L and radius a. Eq. (1) extends into

$$U = \frac{1}{2}ka^2\int_{-\frac{L}{2}}^{\frac{L}{2}}\int_{-\frac{L}{2}}^{\frac{L}{2}}\int_0^{2\pi}\int_0^{2\pi}\frac{\sigma(z)\,\sigma(z')\,\mathrm{d}\varphi'\,\mathrm{d}\varphi\,\mathrm{d}z'\,\mathrm{d}z}{|\boldsymbol{r}-\boldsymbol{r}'|}, \tag{2}$$

where

$$\begin{aligned}|\boldsymbol{r}-\boldsymbol{r}'| &= \sqrt{(z-z')^2+2a^2\left[1-\cos(\varphi-\varphi')\right]}\\ &= \sqrt{(z-z')^2+4a^2\sin^2\frac{\varphi-\varphi'}{2}}.\end{aligned} \tag{3}$$

The surface charge density is assumed in the following form,

$$\sigma(z) = \frac{Q\,s}{2\pi aL}\left[\frac{1}{\sqrt{1-\left(\frac{2z}{L}\right)^2}}+\sum_{n=0}^{N}c_nP_{2n}\left(\frac{2z}{L}\right)\right],\quad -\frac{L}{2}\le z\le\frac{L}{2}. \tag{4}$$

The scaling factor s is applied in order to keep the total charge Q the same. Here, $P_{2n} = P_{2n}^0$ are the Legendre polynomials of the first kind and order $2n$, c_n are the coefficients to be found. Introducing new variables $\mu = \frac{2z}{L}$, $\eta = \frac{\varphi}{2}$, $\rho = \frac{r}{a}$, and a parameter $\xi = \frac{a}{L}$, σ and U become

$$\widetilde{\sigma}(\mu) = \sigma\left(\frac{1}{2}L\mu\right) = \frac{Q\,s}{2\pi\xi L^2}\left[\frac{1}{\sqrt{1-\mu^2}}+\sum_{n=0}^{N}c_nP_{2n}(\mu)\right], \tag{5}$$

$$U = k\,\xi^2L^3\int_{-1}^{1}\int_{-1}^{1}\int_0^{\pi}\int_0^{\pi}\frac{\widetilde{\sigma}(\mu)\,\widetilde{\sigma}(\mu')\,\mathrm{d}\eta'\,\mathrm{d}\eta\,\mathrm{d}\mu'\,\mathrm{d}\mu}{\sqrt{(\mu-\mu')^2+16\xi^2\sin^2(\eta-\eta')}}. \tag{6}$$

Integration over η and η' can be performed analytically, and we can write

$$U = k\,\xi^2L^3\int_{-1}^{1}\int_{-1}^{1}\widetilde{\sigma}(\mu)\,\widetilde{\sigma}(\mu')\,G(\mu,\mu')\,\mathrm{d}\mu'\,\mathrm{d}\mu \tag{7}$$

where G is

$$G(\mu,\mu') = \frac{2\pi K\left(-\frac{16\xi^2}{(\mu-\mu')^2}\right)}{|\mu-\mu'|}. \tag{8}$$

K is the complete elliptic integral of the first kind.

The total charge Q is given by

$$Q = \int_{-\frac{L}{2}}^{\frac{L}{2}}\int_0^{2\pi}\sigma(z)\,a\,\mathrm{d}\varphi\,\mathrm{d}z = \xi L^2\int_{-1}^{1}\int_0^{\pi}\widetilde{\sigma}(\mu)\,\mathrm{d}\eta\,\mathrm{d}\mu \tag{9}$$

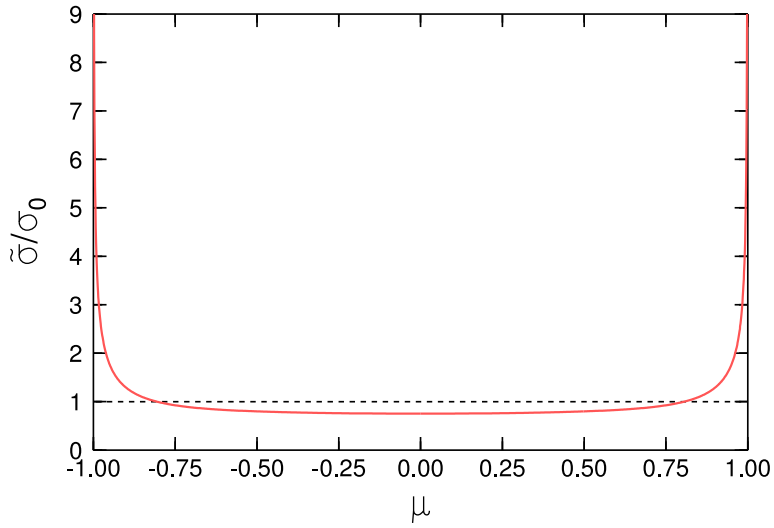

Fig. 2. The dependence of the charge density on $\mu = 2z/L$. The level 1 corresponds to uniform distribution σ_0 of the charge, $\sigma_0 = Q/(2\pi aL)$.

and must be constant. It follows that

$$s = \frac{2}{2c_0 + \pi}. \tag{10}$$

So we have for U

$$U = \frac{kQ^2}{\pi^2 L(2c_0+\pi)^2}\int_{-1}^{1}\int_{-1}^{1}\left[\frac{1}{\sqrt{1-\mu^2}} + \sum_{n=0}^{N} c_n P_{2n}(\mu)\right] \times \left[\frac{1}{\sqrt{1-\mu'^2}} + \sum_{n=0}^{N} c_n P_{2n}(\mu')\right] G(\mu,\mu')\,\mathrm{d}\mu'\,\mathrm{d}\mu. \tag{11}$$

The minimum U condition is used for finding the coefficients c_n. Their determination is described in Appendix.

3. Results

The model presented in Section 2 can be used with any value of ξ. Numerical results will be shown here for $\xi = 0.1$. The charge density $\widetilde{\sigma}$ is found to be:

$$\widetilde{\sigma} = \frac{Q}{2\pi aL}\left(0.0877936\mu^6 - 0.201515\mu^4 - 0.102569\mu^2 + 0.206151 + \frac{0.544819}{\sqrt{1-\mu^2}}\right). \tag{12}$$

The $\widetilde{\sigma}$ is shown in Fig. 2.

The self-energy given by Eq. (11) is

$$U = 79.606\,k\,\frac{Q^2}{4\pi^2 L}\quad, \tag{13}$$

while for the uniformly distributed charge from Eq. (6) by setting $\sigma = \frac{Q}{2\pi\xi L}$ would be

$$U = 83.621\,k\,\frac{Q^2}{4\pi^2 L}\quad. \tag{14}$$

The difference is about 5 percent.

The electrical potential is given by

$$V(\mathbf{r}) = k\int_{Q'}\frac{\mathrm{d}Q'}{|\mathbf{r}-\mathbf{r}'|} \tag{15}$$

where $\mathbf{r}$ is a general point in space and $\mathbf{r}'$ is a point on the cylinder, so that

$$|\mathbf{r}-\mathbf{r}'| = \frac{L}{2}\sqrt{(\mu-\mu')^2 + 4\xi^2(\rho-1)^2 + 16\xi^2\rho\sin^2(\eta-\eta')} \tag{16}$$

and

$$V(\rho,\mu) = \frac{2kQ}{\pi L(2c_0+\pi)} \times \int_0^{\pi}\int_{-1}^{1}\frac{\frac{1}{\sqrt{1-\mu'^2}} + \sum_{n=0}^{N} c_n P_{2n}(\mu')}{\sqrt{(\mu-\mu')^2 + 4\xi^2(\rho-1)^2 + 16\xi^2\rho\sin^2\eta'}}\,\mathrm{d}\mu'\,\mathrm{d}\eta'. \tag{17}$$

V does not depend on η due to symmetry. It remains constant along the cylinder with good accuracy, which can be seen in Fig. 3.

Dependence of self-energy on ξ is depicted in Fig. 4, along with the capacitance C.

For the same total charge, the capacitance is inversely proportional to U. There is an approximation for C in the limit $\xi \to 0$ [20]:

$$C = \frac{L}{2\,k}\,\frac{1}{\ln\left(\frac{2}{\xi}\right) - 1}.$$

The approximation nearly coincides with our results for $\xi < 0.1$ which is demonstrated in Fig. 4. The capacitance obtained with the new solution is in good agreement with Lekner [15].

The electric field components are calculated from $\mathbf{E} = -\nabla V$. Because of symmetry, only E_ρ and E_μ are non-zero components here:

$$E_\rho = -\frac{1}{h_\rho}\frac{\partial V}{\partial \rho},\quad E_\eta = 0,\quad E_\mu = -\frac{1}{h_\mu}\frac{\partial V}{\partial \mu}. \tag{18}$$

The Lamé coefficients of our coordinate system ρ, η, and μ are used, $h_\rho = a$, $h_\eta = 2a\rho$, and $h_\mu = L/2$.

Explicit formulas for the electric field components are

$$E_\rho = \frac{8\xi kQ}{\pi L^2(2c_0+\pi)} \times \int_0^{\pi}\int_{-1}^{1}\frac{(\rho-1+2\sin^2\eta')\left[\frac{1}{\sqrt{1-\mu'^2}} + \sum_{n=0}^{N} c_n P_{2n}(\mu')\right]}{\left[(\mu-\mu')^2 + 4\xi^2(\rho-1)^2 + 16\xi^2\rho\sin^2\eta'\right]^{3/2}}\,\mathrm{d}\mu'\,\mathrm{d}\eta', \tag{19}$$

$$E_\mu = \frac{4kQ}{\pi L^2(2c_0+\pi)} \times \int_0^{\pi}\int_{-1}^{1}\frac{(\mu-\mu')\left[\frac{1}{\sqrt{1-\mu'^2}} + \sum_{n=0}^{N} c_n P_{2n}(\mu')\right]}{\left[(\mu-\mu')^2 + 4\xi^2(\rho-1)^2 + 16\xi^2\rho\sin^2\eta'\right]^{3/2}}\,\mathrm{d}\mu'\,\mathrm{d}\eta'. \tag{20}$$

The electric field component profiles are shown in Figs. 5–7.

We show in Fig. 8 that the coefficient c_0 is close to zero for large ξ and gradually increases with a decreasing ξ. It was found that the surface charge density at $z = 0$ demonstrates a similar dependence on ξ.

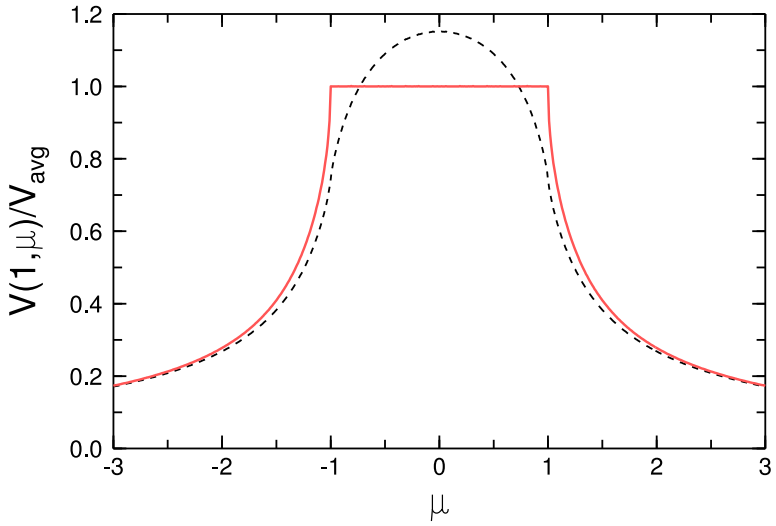

Fig. 3. Dependence of the electrical potential V (red line) at the cylinder and beyond on $\mu = 2z/L$. that is $r = a = \xi L$. The value 1 corresponds to the average value ($V_{\rm avg}$) of V at the cylinder. The dashed line shows the profile of V for the uniformly distributed charge.

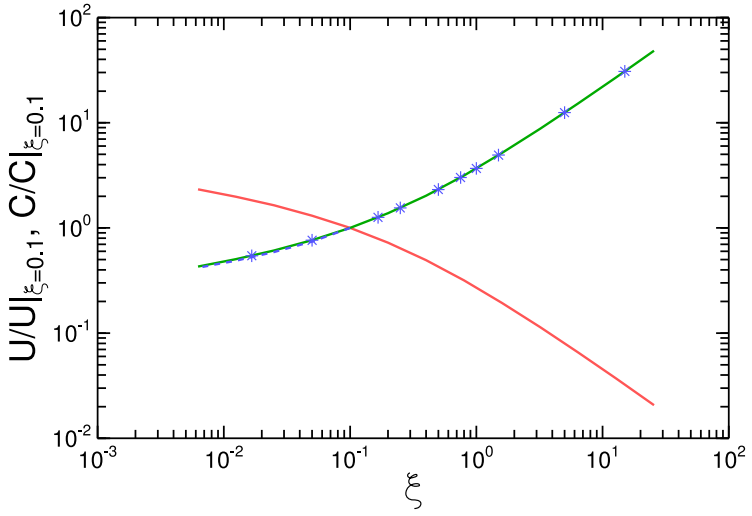

Fig. 4. Dependence of the electrical potential energy U (red line) and capacitance C (green line) on ξ. They are drawn relatively to their values at $\xi = 0.1$. The dashed blue line depicts Maxwell's approximate capacitance formula for very small values of ξ. The blue asterisks represent the Lekner [15] values. (For interpretation of the references to color in this figure legend, the reader is referred to the web version of this article.)

The equipotential contours of electric potential are shown in Fig. 9, while those of the electric field magnitude in Fig. 10.

It is possible to plot field lines in the xz plane using Euler potentials (Romashets and Vandas, 2011), because of axial symmetry. There are two benefits of using Euler potentials for the field lines. The first is to avoid numerical errors which may happen in field line tracing. Second, the field lines density is calibrated by the flux and one can see the increase and decrease of the electric field magnitude from the lines density. The electrical field in the region not occupied by the charges, that is where $\nabla\cdot\mathbf{E} = 0$, inside and outside of the cylinder, is represented as

$$\mathbf{E} = \nabla\alpha \times \nabla\beta, \tag{21}$$

where α and β are the Euler potentials [22]. We can set $\beta = \eta$. Then α is determined using Eq. (21), from which it follows that

$$E_\rho = -\frac{1}{h_\mu h_\eta}\frac{\partial\alpha}{\partial\mu} \quad \Rightarrow \quad \alpha = -\int h_\mu h_\eta E_\rho \,\mathrm{d}\mu. \tag{22}$$

Using Eq. (22), we have

$$\alpha(\rho,\mu) = -\frac{8\xi^2 kQ\rho}{\pi(2c_0+\pi)} \times \int_0^{\mu}\int_{-1}^{1}\int_0^{\pi} \frac{(\rho - 1 + 2\sin^2\eta')\left[\frac{1}{\sqrt{1-\mu'^2}} + \sum_{n=0}^{N} c_n P_{2n}(\mu')\right]}{\left[(\mu''-\mu')^2 + 4\xi^2(\rho-1)^2 + 16\xi^2\rho\sin^2\eta'\right]^{3/2}} \,\mathrm{d}\eta'\,\mathrm{d}\mu'\,\mathrm{d}\mu''. \tag{23}$$

The integration over μ' and μ'' can be done analytically.

In the plane xz (i.e., $\eta = 0$ and $\frac{\pi}{2}$), the field lines are contour lines of $\alpha = \text{const}$. This method of drawing α contour lines is more reliable than tracing the lines with Eq. (22), because it avoids possible numerical errors.

The integration over μ'' yields (see the Eq. (24) in Box I).

The electric field lines are shown in Fig. 11 as contour lines of α.

4. Capacitance

Analysis of electric potential V_0 on the cylinders with the same charge Q and different $\xi = \frac{a}{L}$ leads to a dependence on ξ, which can be described in terms of a function f,

$$V_0 = \frac{kQ}{\pi L} f(\zeta), \tag{25}$$

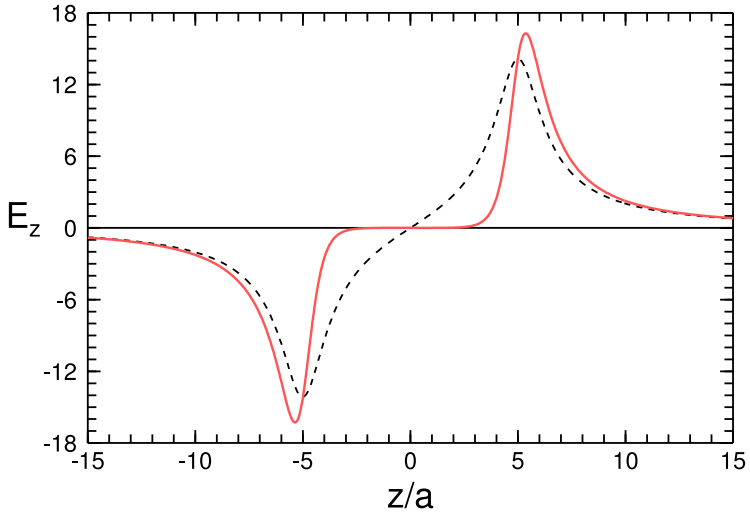

Fig. 5. Dependence of the z-component of the electric field (red line, in ad-hoc units) along the axis of the cylinder. The dashed line shows the same for the uniformly distributed charge. The cylinder occupies the interval $\langle -5, 5\rangle$ in the plot.

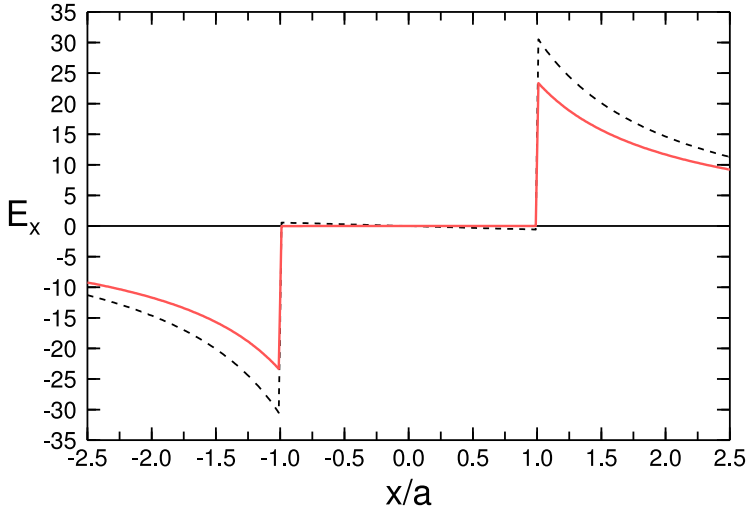

Fig. 6. Dependence of the x-component of the electric field (red line) along the line perpendicular to the axis of the cylinder, which passes through the origin (ad-hoc units but the same as in Fig. 5). The dashed line shows the same for the uniformly distributed charge. The cylinder occupies the interval $\langle -1, 1\rangle$ in the plot.

$$\alpha = \frac{8k\xi^2 Q}{\pi^2 + 2\pi c_0} \int_{-1}^{1}\int_{0}^{\pi} \frac{(\mu' - \mu)\rho(\rho - 1 + 2\sin^2\eta')\left[\frac{1}{\sqrt{1-\mu'^2}} + \sum c_n P_{2n}(\mu')\right] \mathrm{d}\eta'\,\mathrm{d}\mu'}{\left[\xi^2(\rho-1)^2 + 4\xi^2\rho\sin^2\eta'\right]\sqrt{(\mu-\mu')^2 + 4\xi^2(\rho-1)^2 + 16\xi^2\rho\sin^2\eta'}}. \tag{24}$$

Box I.

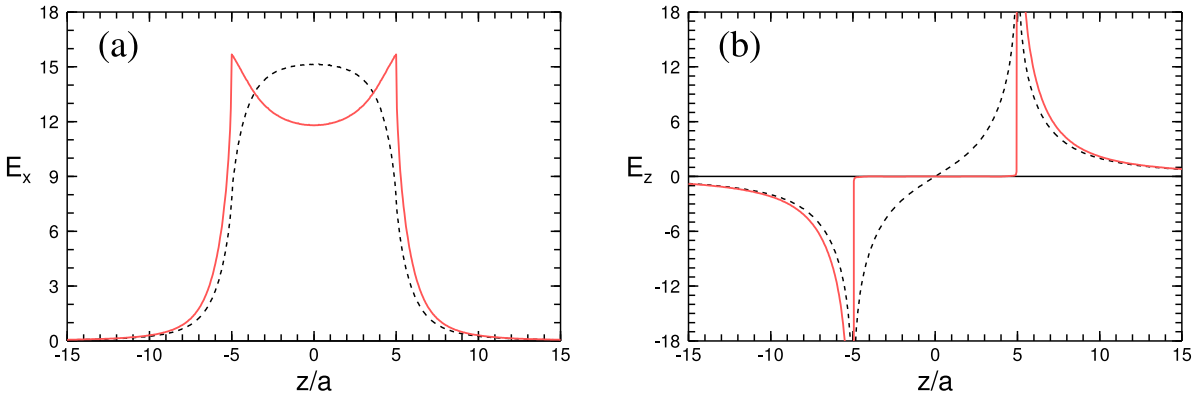

Fig. 7. Dependence of (a) the x-component and (b) the z-component of the electric field (red lines) along the line $x = a$ (ad-hoc units but the same as in Figs. 5–6). The dashed line shows the same for the uniformly distributed charge. The cylinder occupies the interval $\langle -5, 5\rangle$ in the plots.

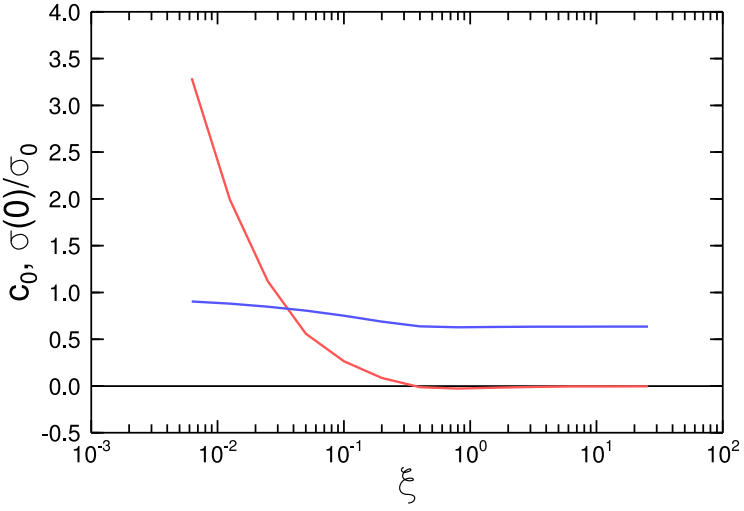

Fig. 8. Dependence of the charge density at $z = 0$ (blue line) and the coefficient c_0 (red line) on ξ. For the charge density, the level 1 corresponds to the uniform charge distribution. (For interpretation of the references to color in this figure legend, the reader is referred to the web version of this article.)

$$C = \frac{\pi L}{k}\,\frac{1}{\frac{0.0205\tanh(8.1-3\zeta)+0.0205}{\left(0.0000153554|\zeta-6.5|^{4.2}+0.009\right)^{1.3}} + 3.05607(\zeta-0.955856)\{\tanh[3(\zeta-2.7)]+1\}}, \tag{27}$$

Box II.

where $\zeta = \ln\frac{2}{\xi}$. The function is depicted in Fig. 12.

It is given by

$$f = \frac{0.0205\tanh(8.1-3\zeta)+0.0205}{\left(0.0000153554|\zeta-6.5|^{4.2}+0.009\right)^{1.3}} + 3.05607(\zeta-0.955856)\{\tanh[3(\zeta-2.7)]+1\}. \tag{26}$$

The capacitance in closed form is found to be (see the Eq. (27) in Box II) and it provides a good agreement with the model, for small and large ξ.

5. Conclusions

A solution of the surface charge density distribution of a finite length, radius, and zero-thickness conducting cylinder is found. It is used for the calculation of self-energy, electric potential and field, and capacitance in a closed form. The least squares method was applied in order to find the minimum potential energy state. Basic functions were the Jackson [21] term and Legendre polynomials of even power. The results show that the charge density provides a constant voltage on the cylinder.

Declaration of competing interest

The authors declare that they have no known competing financial interests or personal relationships that could have appeared to influence the work reported in this paper.

Data availability

No data was used for the research described in the article.

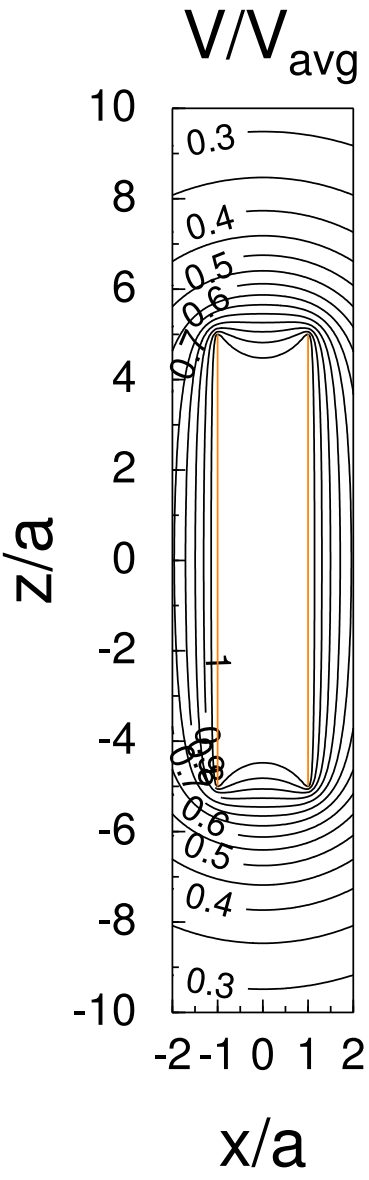

Fig. 9. Contour lines V, calculated using Eq. (17), in the xz plane. They are scaled by V_{avg}, the same as in Fig. 3. The red lines show the extension of the cylinder. They follow the contour line labeled by 1. (For interpretation of the references to color in this figure legend, the reader is referred to the web version of this article.)

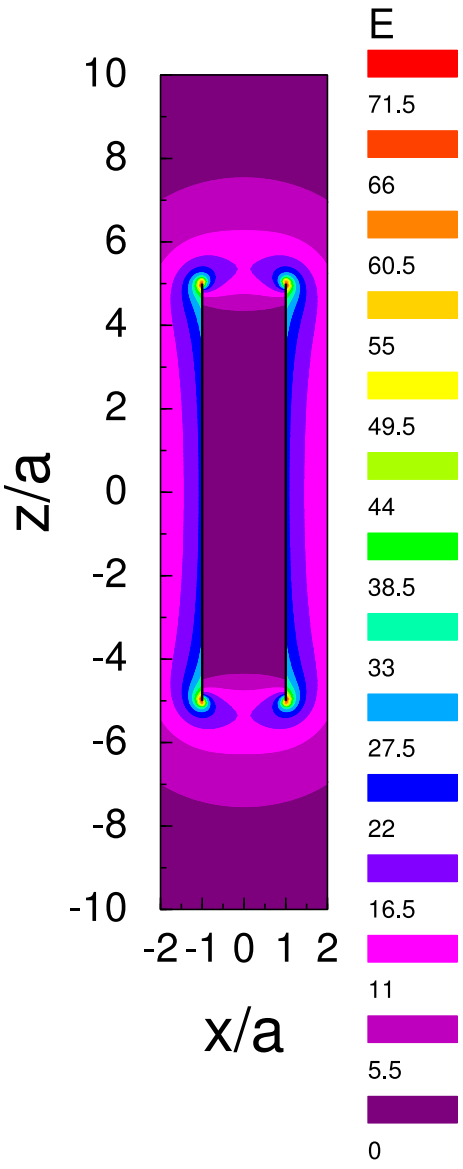

Fig. 10. Contour plot of electric field magnitude E, calculated using Eqs. (19)–(20), in the xz plane. E is plotted in ad-hoc units but the same as in Figs. 5–7. The extension of the cylinder is shown by thicker black lines. (For interpretation of the references to color in this figure legend, the reader is referred to the web version of this article.)

Acknowledgments

This research was supported by the NSF, USA grant 2230363. M. V. acknowledges support from the AV ČR, Czech Republic grant RVO:67985815.

Appendix

Eq. (11) is symbolically rewritten into the form

$$U = \frac{kQ^2}{\pi^2 L}\,\frac{c_0^2 I_{00} + 2c_0\left(\sum_{n=1}^{N} c_n I_{0n} + I_0\right) + \sum_{n=1}^{N}\sum_{m=1}^{N} c_n c_m I_{nm} + 2\sum_{n=1}^{N} c_n I_n + I}{(2c_0+\pi)^2} \tag{A.1}$$

where

$$I_{nm} = \int_{-1}^{1}\int_{-1}^{1} P_{2n}(\mu)\,P_{2m}(\mu')\,G(\mu,\mu')\,\mathrm{d}\mu'\,\mathrm{d}\mu, \tag{A.2}$$

$$I_n = \int_{-1}^{1}\int_{-1}^{1} \frac{P_{2n}(\mu)\,G(\mu,\mu')}{\sqrt{1-\mu^2}}\,\mathrm{d}\mu'\,\mathrm{d}\mu, \tag{A.3}$$

$$I = \int_{-1}^{1}\int_{-1}^{1} \frac{G(\mu,\mu')\,\mathrm{d}\mu'\,\mathrm{d}\mu}{\sqrt{(1-\mu^2)(1-\mu'^2)}}. \tag{A.4}$$

It holds $I_{nm} = I_{mn}$ because the integrand is symmetric with respect to μ and μ'.

For U to be a minimum, it must hold

$$\frac{\partial U}{\partial c_n} = 0, \qquad n = 0, \ldots, N. \tag{A.5}$$

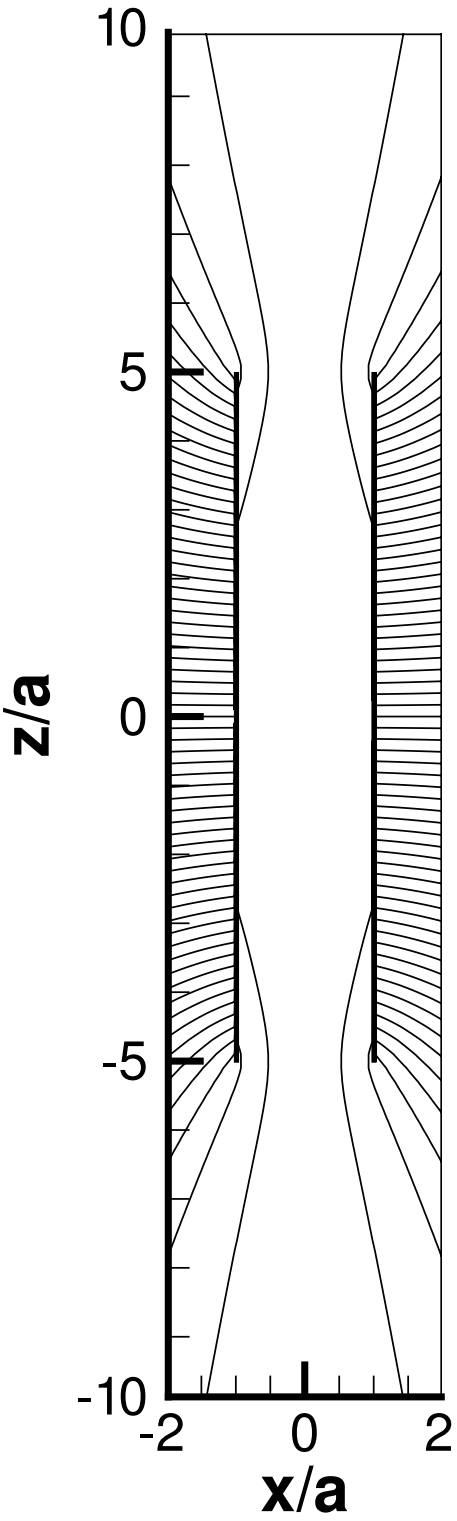

Fig. 11. Electric field lines drawn as α contour lines. The extension of the cylinder is shown by thicker black lines.

Eq. (A.5) yields for $n = 0$

$$c_0 = \frac{2\sum_{n=1}^{N}\sum_{m=1}^{N} c_n c_m I_{nm} + 4\sum_{n=1}^{N} c_n I_n + 2I - \pi\sum_{n=1}^{N} c_n I_{0n} - \pi I_0}{\pi I_{00} - 2\sum_{n=1}^{N} c_n I_{0n} - 2I_0}, \tag{A.6}$$

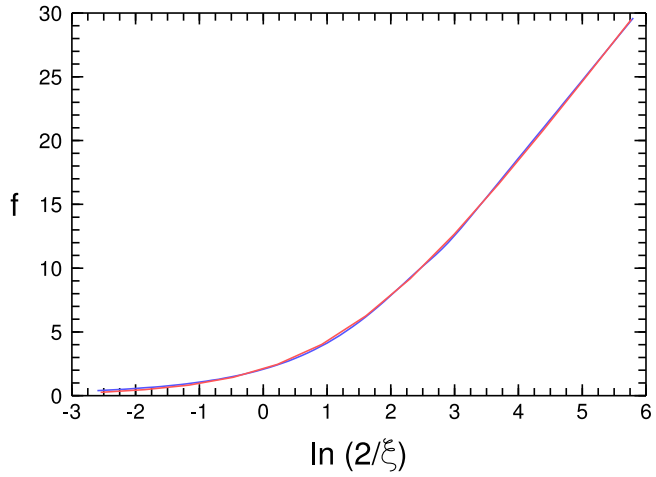

Fig. 12. The f from Eq. (25) as a function of $\ln(2/\xi)$. Blue line – formula, red – calculations from self-energy. (For interpretation of the references to color in this figure legend, the reader is referred to the web version of this article.)

and for $n > 0$

$$\sum_{m=1}^{N} c_m I_{nm} = -I_{0n} c_0 - I_n. \tag{A.7}$$

The coefficients are determined by an iteration. With known c_n, $n > 0$, Eq. (A.6) provides c_0 (in the beginning we set $c_n = 0$ for $n > 0$). This c_0 is substituted into Eq. (A.7) which then represents a system of linear equations for the remaining c_n. These c_n are used in Eq. (A.6) and the procedure repeats until a prescribed precision of the coefficients is achieved. We get the following set of coefficients: $c_0 = 0.264676$, $c_1 = -0.260131$, $c_2 = -0.0343165$, $c_3 = 0.0111614$.

References

[1] L.D. Landau, E.M. Lifshitz, Electrodynamics of Continuous Media, Pergamon, New York, 1984.
[2] M.X. Yang, F. Yang, Electric analysis of a conducting hemisphere, J. Phys. D 49 (2016) 175501.
[3] J. Batle, O. Ciftja, M. Naseri, M. Ghoranneviss, K. Nagata, T. Nakamura, Coulomb self-energy integral of a uniformly charged d-cube: A physically-based method for approximating multiple integrals, J. Electrost. 85 (2017) 52–60, http://dx.doi.org/10.1016/j.elstat.2016.12.008.
[4] O. Ciftja, A result for the Coulomb electrostatic energy of a uniformly charged disk, Results Phys. 7 (2017) 1674–1675.
[5] D.J. Griffiths, Y. Li, Charge density on a conducting needle, Am. J. Phys. 64 (1996) 706–714.
[6] J.D. Jackson, Charge density on a thin straight wire, revisited, Am. J. Phys. 68 (2000) 789–799.
[7] O.F. de Alcantara Bonfim, D. Griffiths, Comment on charge density on a thin straight wire, revisited, by J.D. Jackson [Am. J. Phys. 68 (9), 789–799 (2000)], Am. J. Phys. 69 (2001) 515–516.
[8] A.A. Bruno, J.R. Brauder, Scattering from an infinite, finitely conducting cylinder by finite element analysis, J. Appl. Phys. 63 (1988) 3200–3202.
[9] J.R. Wait, D.A. Hill, Excitation of a homogeneous conductive cylinder of finite length by a prescribed axial current distribution, Radiol. Sci. 8 (1973) 1169–1176.
[10] J.A. Hernandes, A.K.T. Assis, Electric potential due to an infinite conducting cylinder with internal or external point charge, J. Electrostat. 63 (2005) 1115–1131.
[11] R.W. Sharstein, Capacitance of a tube, J. Electrostat. 65 (2011) 21–29.
[12] A. Weinheimer, The charge induced on a conducting cylinder by a point charge and its application to the measurement of charge on precipitation, J. Atmos. Ocean Technol. 5 (1988) 298–304.
[13] A. Buikis, H. Kalis, Calculations of electromagnetic fields, forces and temperature in a finite cylinder, Math. Model. Anal. 7 (2002) 21–32.
[14] L. Verolino, Capacitance of a hollow cylinder, El. Eng. 78 (1995) 201–207.
[15] J. Lekner, Electrostatics of Conducting Cylinders and Spheres, AIP, Washington, 2021.
[16] P.L. Kapitsa, V.A. Fok, L.A. Vainshteyn, Static boundary value problem for a hollow cylinder of finite length, Tech. Phys. Sov. Phys. 4 (1960) 1077–1087.

[17] L.A. Vainshteyn, Static boundary value problem for a hollow cylinder of finite length: Part II. Numerical results and part III. Approximate formulas, Tech. Phys. Sov. Phys. 7 (1963) 855–866.
[18] N.N. Lebedev, I.P. Skalskaya, Application of dual integral equations to the electrostatic problem of a hollow conducting cylinder of finite length, Tech. Phys. Sov. Phys. 18 (1973) 28–32.
[19] C.M. Butler, Capacitance of a finite-length conducting cylindrical tube, J. Appl. Phys. 51 (1980) 5607–5609.
[20] J.C. Maxwell, On the electrical capacity of a long narrow cylinder, and of a disk of sensible thickness, Proc. Lond. Math. Soc. 9 (1877) 94–102.
[21] J.D. Jackson, Classical Electrodynamics, second ed., Wiley, New York, 1975.
[22] E.P. Romashets, M. Vandas, Euler potentials for two line currents aligned with an ambient uniform magnetic field, J. Geophys. Res. 116 (A09227) (2011).